Numerical Simulation of Dynamic Behaviour of an Azimuth Thruster in Seaways

Vladimir Krasilnikov[1] **and Nabila Berchiche**[2]
[1]SINTEF Ocean, Trondheim/Norway, [2]formerly SINTEF Ocean
vladimir.krasilnikov@sintef.no

1 Introduction

Operations performed by offshore vessels become increasingly demanding. The recent trend to exploit more exposed sea regions, which we witness in wind energy and aquaculture sectors, means that propulsors installed on such vessels would frequently operate under off-design conditions that may involve large oblique flow angles, ventilation, waves, wave induced ship motions, extreme manoeuvres and impact of slipstream from a neighbouring thruster. The said phenomena are linked to mechanical failures in gears and bearings of azimuth thrusters. They may also result in loss of thrust that can compromise vessel manoeuvring and station keeping performance. Ventilation is identified as one of the most severe phenomena responsible for harmful unsteady load oscillations. Over the last decade a considerable amount of experimental, and more recently, numerical research has been conducted on this topic. In this paper we study numerically the performance of a pushing ducted thruster in regular waves and under the influence of wave-induced planar motions.

2 Impact of ventilation on propulsor performance

According to experimental studies in (Koushan, 2006), the onset of developed ventilation is associated with a sudden drop of thrust and torque and increase of blade load oscillations. For a ducted thruster in bollard operation, at the fixed submergence H/Dp=0.5 (where H is the submergence and Dp is the propeller diameter), without waves, the duct loses about 95% of its thrust, while propeller loses about 80% of its thrust. These figures correlate very well with the magnitudes of thrust losses predicted from CFD analyses carried out on the same propulsor in (Berchiche et al, 2018). Both the measurements and calculations show that blade thrust oscillations increase rapidly already at submergence H/Dp=0.8÷0.7, i.e. when the ventilation event first occurs. The critical submergence and ventilation inception mechanism are shown to be different under the conditions of light loading and heavy loading of propulsor (Berchiche et al, 2018). At light loading such as in transit, fully ventilated condition develops suddenly, in the form of a pocket-like deformation of free surface. At heavy loading such as in bollard or trawling, ventilation reveals an inception stage where a vortex develops from the free surface toward the propulsor, and it serves as an air transport way. There are also distinctly different pictures of air entrainment by propeller blades inside the duct. In regular waves, a sudden drop of thrust occurs at a certain critical advance coefficient, which depends on propulsor loading and submergence (Koushan et al, 2009). In the sub-critical range, the effect of wave height is significant. Maximum thrust losses are registered during the passage of wave troughs where the largest amount of ventilation is found. Blade load amplitudes reach maximum when wave crests pass the propulsor, but the averaged blade thrust at that time is lowest, and vice versa when wave troughs pass. This gives an indication of the influence of wave-induced orbital velocities. Some extreme events such as local peak loads are also registered (Dang et al, 2013). It is hypothesized that these are associated with the collapse of large air pockets.

3 Numerical approach

For the numerical investigation of a generic azimuth ducted thruster whose configuration is detailed in (Koushan, 2006), (Berchiche et al, 2018), an unsteady RANS method of the commercial CFD code STAR-CCM+ (version 12.04) is employed. In order to resolve the interaction between the rotating propeller and stationary components of propulsor such as pod and duct, the mesh region surrounding propeller is separated from the outer fluid (see Fig. 1), and during the solution it participates in rotational motion around propeller shaft axis. The sliding mesh interfaces are applied between the propeller region and outer fluid region. The implicit unsteady solution is performed with a 1st order temporal discretization scheme and the time step corresponding to 1 degree of propeller rotation. Keeping the time step sufficiently small is essential for both the solution stability and accuracy of prediction of unsteady blade loads. The flow is assumed fully turbulent, and the SST k-ω model with "All Y+" near-wall modelling algorithm is used for turbulence closure. The two-phase fluid is considered using the Eulerian Multiphase Mixture model with the VOF method. The High-Resolution Interface Capturing (HRIC) scheme is used for tracking the water-air interface. The default settings of the HRIC scheme in STAR-CCM+ are adopted (2nd order convection scheme, sharpening factor 0.0, angle factor 0.5, CFL_l=0.5, CFL_u=1.0). No phase interaction and phase change are allowed in the solution, so that cavitation is not modelled in the problems with free surface, even though it would develop in a realistic flow, under simulated conditions. For modelling regular waves, a 5th order VOF Wave model is used with wave height, wave period, wave velocity and wave direction specified. The waves are assumed to arrive on the propulsor from ahead and their speed equals to the speed of advance of propulsor. The 2nd order discretization scheme is used in the VOF method.

A large rectangular computation domain (X×Y×Z=200Dp×200Dp×40Dp) is used in the present model to accommodate a sufficient number of wave lengths in the simulations of propulsor in regular waves, and to avoid the influence of boundaries in oblique flow calculation. With the domain of this size, no additional treatment of wave setup is usually required, unless the simulated waves are very long. In the latter scenarios, wave forcing at the outlet boundary is recommended. For modelling the general case that may involve wave-induced planar motions of propulsor and propulsor azimuthing, the two different approaches were investigated – the moving mesh method and overset mesh method. The moving mesh setup contains the two regions – the stationary fluid region and rotating (sliding mesh) propeller region. In the case of forced propulsor motion, the whole region of stationary fluid participates in that motion. In the overset mesh setup, we add one more region – the overset region that surrounds the propulsor and moves according to the user defined motion. In this method, the background fluid region is always stationary, while propeller region is rotating, as before, with respect to the outer (overset) region. The mesh refinement patterns are very similar in the two methods. Some illustrations of mesh refinement are shown in Fig. 1 and 2.

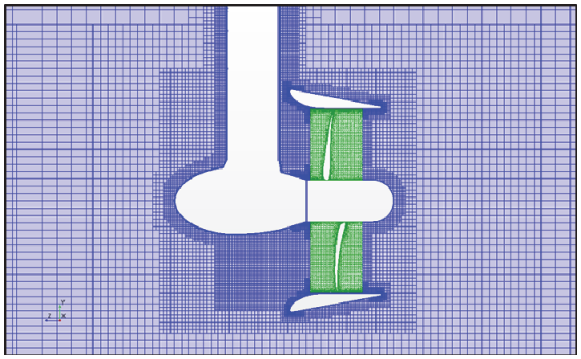

Fig.1: Mesh refinement around propulsor.

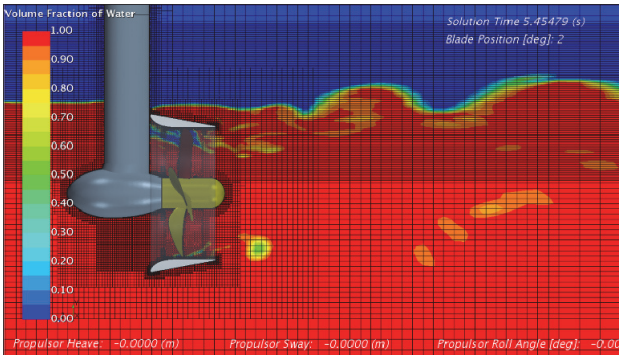

Fig.2: Mesh refinement near free surface.

The important areas that require mesh refinement are the region around propulsor (cell size 1% of Dp), wake area downstream of the strut (cell size 0.5% of Dp), duct leading and trailing edges, propeller blade tip clearance (cell size 0.25% of Dp), as well as leading and trailing edges of propeller blades (cell size 0.125% of Dp). In presence of waves, 40-50 cells per wave height and 120-160 cells per wave length are recommended for this type of simulations due to strong deformations of free surface, resulting from the interaction between the waves and propulsor and ventilation phenomenon. With the above mesh refinement settings, the total cell count is about 17-18 mil in the problems with initially calm free surface, and about 23-25 mil in the problems with regular waves.

There are different ways to simulate a desired motion of propulsor in STAR-CCM+. The forced planar motions can be set up using the general DFBI Rotation and Translation method with the Planar Motion Carriage option. Within this option, the model "General Planar Motion" is available, where one can prescribe a three-component motion either in the roll plane (heave, sway, roll), or in the pitch plane (heave, surge, pitch), or in the yaw plane (surge, sway, yaw). The alternative to DFBI method is to use the mesh motion method, where the same scenarios can be set as forced translational and rotational motions through the velocity equations, using motion managed coordinate systems.

The results of test calculations with the two motion modelling approaches (moving mesh and overset mesh) and the two motion setup methods (DFBI and mesh motion) are discussed below. Table 1 presents a comparison between the measured and computed characteristics of propulsor operating at the advance coefficient J=0.3 (J=V/n/Dp) in straight flow, without free surface.

Table 1: Comparison of integral propulsor characteristics obtained with different calculation methods. (J=0.3, straight flow, no free surface)

	KTP	KTD	KTG	KTTOT	KQP
EXP	0.3170	0.1830	-0.0490	0.4510	0.0570
Moving mesh / Mesh motion	0.3039	0.1736	-0.0353	0.4421	0.0572
Overset Mesh / Mesh motion	0.3039	0.1737	-0.0354	0.4422	0.0572
Moving mesh / DFBI	0.3011	0.1732	-0.0358	0.4386	0.0571
Overset Mesh / DFBI	0.3009	0.1734	-0.0356	0.4387	0.0570

A good agreement between the solutions obtained with different motion formulations is observed. The computed values also correlate well with the experimental data. The solutions using the DFBI formulation with superposed rotation of propeller region show a slightly lower propeller thrust (about -1.0%) than the solutions using the mesh motion formulation. In the second test case, the propulsor was subject to forced heave motion with the amplitude of 0.5Dp and frequency of 1.1Hz (1/10 of propeller rotation frequency), at the same J=0.3. Fig. 3 and 4 illustrate a comparison between the two mesh motion solutions, according to the DFBI method.

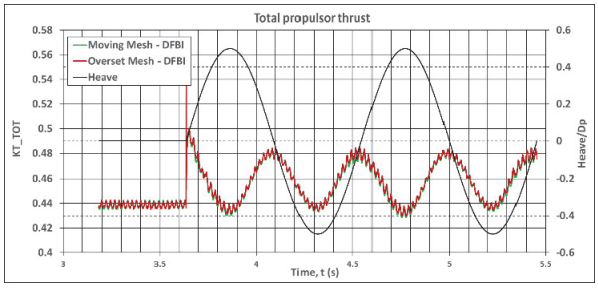

Fig.3: Computed oscillations of total propulsor thrust during heave.

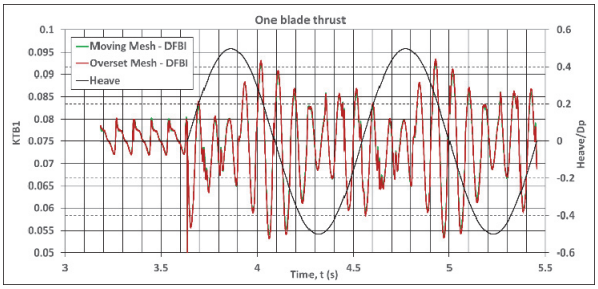

Fig.4: Computed oscillations of single blade thrust during heave.

It can be seen that the moving mesh method and overset mesh method bring nearly identical results. The overset mesh method takes about 1.5 longer time per time step than the moving mesh method due to the update of overset interfaces, in addition to the update of sliding interfaces of propeller region. For further studies in the present work, the moving mesh approach with the DFBI method was employed.

3 Propulsor dynamics in regular waves

The numerical analyses of propulsor in regular waves were performed for the range of wave height (1.0m, 2.5m and 3.0m) and the range of wave period (4s, 8s and 10s), at the transit (J=0.6) and bollard (J=0.0) operation conditions. The simulations were divided into the two groups – the scenarios without ventilation and with ventilation, which were achieved by varying propulsor submergence. The propulsor position with respect to the level of calm free surface was assumed fixed. In the ventilation free conditions at transit, the total thrust of propulsor shows a certain dependency on wave height and period, as illustrated in Fig. 5. For the lowest waves of 1m height, there is no significant dependency of thrust on wave period, while the thrust value is reduced for about 1% compared to the case without waves, at the same submergence. For higher waves, propulsor thrust decreases with the decrease of wave period, and in 3m waves with the period of 4s thrust loss of 5% is predicted. The main contribution to the thrust loss comes from the reduction of duct thrust, which is caused by changes in pressure distribution over the exterior side of the duct under the influence of passing waves.

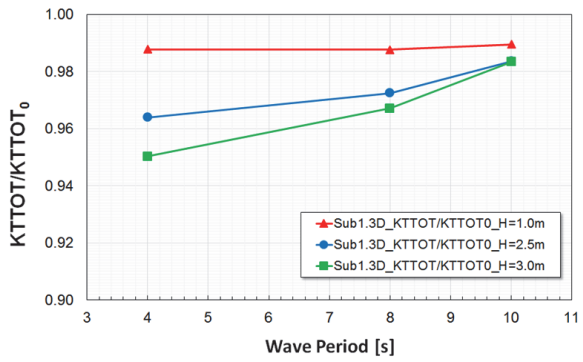

Fig.5: Influence of wave height and period on total propulsor thrust. Transit, J=0.6, H/Dp=1.3, no ventilation. $KTTOT_0$ is the reference value at the same submergence without waves.

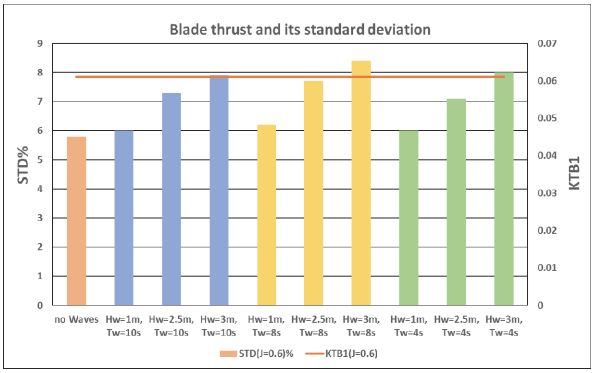

Fig.6: Influence of wave height and period on the amplitude of single blade thrust. Transit, J=0.6, H/Dp=1.3, no ventilation. STD shows standard deviation from mean values.

The averaged value of blade thrust is little affected by the wave period and wave height. However, for the given wave period, the amplitudes of blade thrust oscillations increase with the increase of wave height, as shown in Fig. 6. During bollard operation, at submergences where ventilation does not occur, the influence of regular waves does not result in significant reduction of thrust, while single blade thrust demonstrates similar trends with the variation of wave height and period.

The onset of ventilation event on propulsor in regular waves depends on propulsor loading, submergence and wave parameters. Its impact on total propulsor thrust in transit operation is illustrated in Fig. 7. In longer waves with periods 10s and 8s, intermittent ventilation is found whose cycles occur only for a certain period of time during the passage of wave troughs. The thrust losses amount 2% and 5%, respectively. In shorter waves with period 4s, ventilation is a continuous event, and it results in thrust losses of about 16%. While in longer waves there is dependency of thrust loss on wave height, it is not evident in shortest waves.

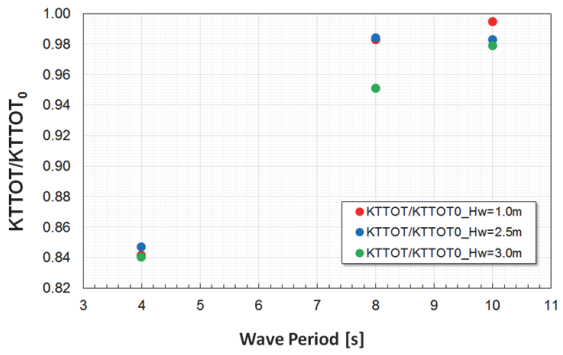

Fig. 7: Thrust losses on propulsor in transit operation in regular waves with ventilation. J=0.6, H/Dp=1.0. $KTTOT_0$ is the reference value at the same submergence without waves.

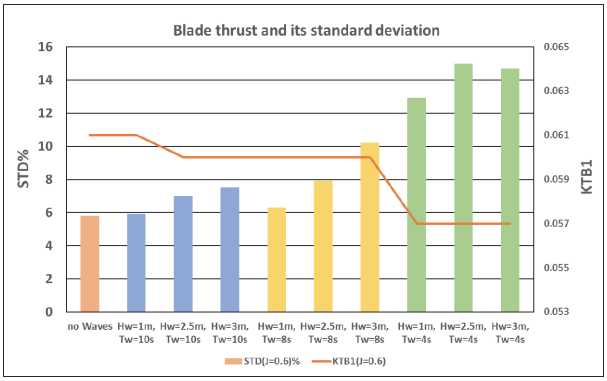

Fig. 8: Influence of wave height and period on the amplitude of single blade thrust with ventilation. Transit, J=0.6, H/Dp=1.0. STD shows standard deviation from mean values.

Fig. 8 illustrates the influence of ventilation on the amplitudes of single blade thrust, for the same conditions. It can be seen that, while the averaged value of blade thrust shows only minor changes, the amplitudes of blade thrust oscillation increase considerably when ventilation occurs. The said increase is especially pronounced in short waves, Tw=4s. The time histories of blade thrust and duct thrust are presented for the case of 3m waves of different periods in Fig. 9 and 10, respectively.

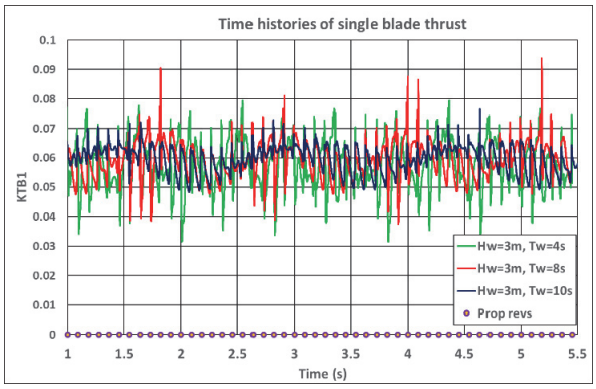

Fig. 9: Time histories of single blade thrust during transit operation in 3m regular waves with the occurrence of ventilation. J=0.6, H/Dp=1.0.

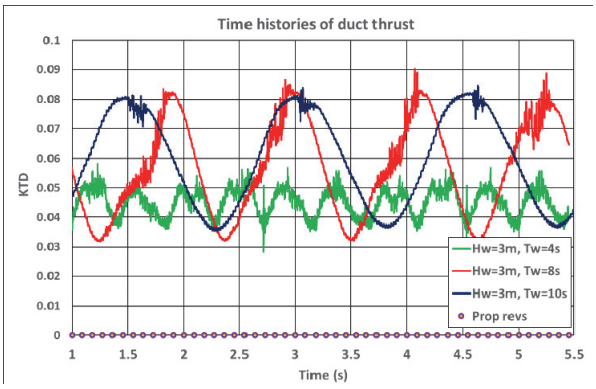

Fig. 10: Time histories of duct thrust during transit operation in 3m regular waves with the occurrence of ventilation. J=0.6, H/Dp=1.0.

In the waves of 10s period, where only a very short ventilation event is found, both the duct thrust and blade thrust show a sinusoidal pattern. Their values increase when the wave trough is approaching. After the brief ventilation event, which is marked by "spikes" in the duct thrust curve, the thrust values begin to decrease, reaching their minima when the crest arrives. Blade thrust oscillations are higher after the passage of wave trough. In the waves of 8s period, the approach of wave trough is marked by the ventilation on the duct, and eventually on propeller. It is noticed in blade thrust history from a rapid increase of oscillation amplitudes. The largest load gradients correspond to the instances when the blade enters the air pockets. The last phase of ventilation, right after the trough passage, is marked by sudden local peaks of blade loads, which are caused by the collapse of air pocket inside the duct. At these instances, the full amplitude of blade thrust oscillation may reach 75% of averaged value. In shortest waves of 4s period, ventilation is a continuous event. The duct thrust is reduced significantly, since the upper part of the duct is always affected by air fraction. The blade thrust

reveals large oscillations with the amplitude about 50% of averaged values, as the blade goes through the air pocket that stays in the upper part of propeller disk.

The development of ventilation on propulsor in regular waves reveals distinct differences between the conditions of light loading operation and heavy loading operation. As one can see from Fig. 11, in the case of transit, for a given wave height ventilation starts earlier in shorter waves, while in bollard it starts earlier in longer waves. This result is explained by the different ventilation inception mechanisms at light loading and heavy loading. In regular waves, the important factor is the exposure time of propulsor to passing wave troughs. Free surface pockets that lead to propulsor ventilation at light loading tend to become more stable in shorter waves, so that the ventilation condition is easier to establish. On the contrary, at heavy loading the vortices which develop from free surface along the strut and which conduct air to propulsor tend to become more stable in longer waves. A more in-depth discussion about the mentioned phenomena can be found in (Krasilnikov et al, 2019).

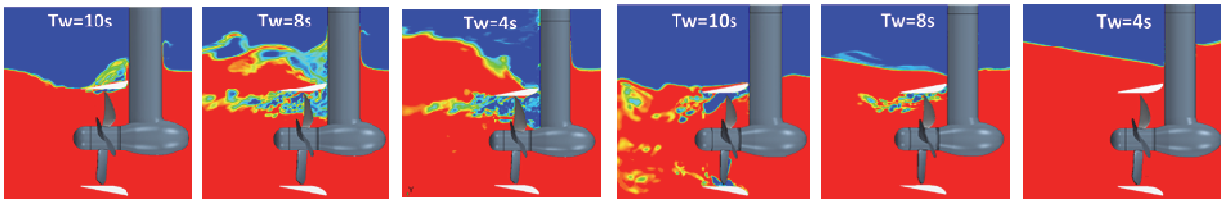

a) Transit, J=0.6, H/Dp=1.0 b) Bollard, J=0.0, H/Dp=1.1

Fig. 11: Ventilation extent on propulsor in regular waves of 3m height with different periods. Transit and bollard operation conditions.

4 Propulsor dynamics at forced planar motions

In the present study the focus was on low speed operation. The cases of trawling (J=0.3) and bollard (J=0.0) were considered, firstly, without the influence of free surface. Simulation scenarios included separate heave, sway and roll motions as well as their combination. The parameters of propulsor motions were derived from the calculation of RAOs at the location of propeller center for a typical offshore vessel, operating in regular waves with the height of 2.5m and period of 8s. The heave and sway motions had approximately the same phase, while roll motion had a phase shift of about -20 deg with respect to heave and sway. With the given conditions, propeller performed about 29 revolutions during one complete propulsor oscillation. Three propulsor oscillations were simulated and the results were sampled from the last two oscillations. The time histories of total propulsor thrust at different planar motions are presented in Fig. 12 and 13, for the cases of trawling and bollard operation, respectively. At trawling, the propulsor thrust experiences largest oscillations during the combined motion. The major contribution comes from the duct thrust variation due to the heave motion component. In addition to large low frequency oscillations directly related to propulsor motion, there are also found high frequency oscillations caused by the interaction of propeller blades with the domains of separated flow behind the pod housing. In the case of combined motion, the changes in loads on propulsor components are not the result of simple addition of changes experienced separately during heave, sway and roll. This gives one an indication that hydrodynamic interaction between the motion components is important. When propeller is moving upwards and passes the position of zero heave, the duct thrust reaches its maximum, and hence the propeller experiences highest flow acceleration by the duct. It results in the occurrence of pressure side cavitation on propeller blades, which is not present when propulsor operates at the same advance coefficient at a fixed position. Unlike trawling operation, in bollard the sway motion and combined motion show comparable amplitudes of oscillations at the motion frequency. The variation of duct thrust and propeller thrust due to sway are the major contributors.

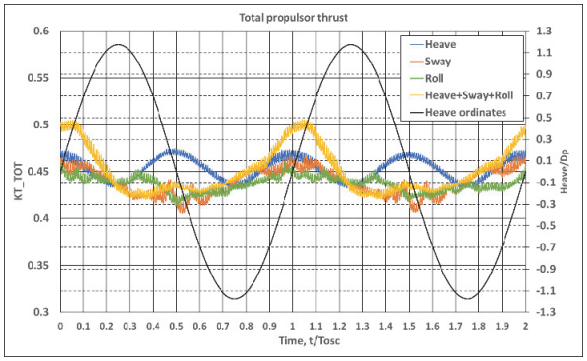

Fig. 12: Time histories of total propulsor thrust at different planar motions. Trawling, J=0.3.

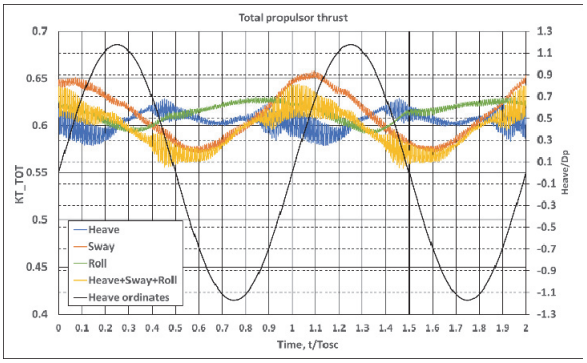

Fig. 13: Time histories of total propulsor thrust at different planar motions. Bollard, J=0.0.

The oscillations at blade passing frequency are still caused by heave, and they reveal larger amplitudes than those at trawling. This is the result of flow separation on the interior side of the duct, which does not develop when propulsor is moving with some, while low speed, but which takes place at zero speed due to very large angles of attack experienced by the duct sections during heave. This separation phenomenon also results in increase of blade loading and cavitation extents on propeller blades when they pass through the separation zone. In general, cavitation is more severe during bollard. In addition to propeller blades, it is also found on the duct leading edge, and it reveals a more dynamic behaviour.

5 Conclusions

CFD provides a useful framework for the quantification of thrust losses and dynamic loads on propulsors operating in seaways, as well for a better understanding of physical mechanisms underlying these phenomena, their dependency on propulsor loading, operation conditions and scale. The onset of ventilation in regular waves depends on propulsor loading, submergence and wave parameters. Ventilation may develop in intermittent form, or in stable form that exists continuously. It is the continuous ventilation that results in largest thrust losses. However, intermittent form may be the cause of strong oscillations of blade thrust, with amplitudes reaching, under some conditions, 75% of mean value. Different ventilation inception mechanisms at light and heavy propulsor loading, and influence of exposure time to passing wave troughs determine different dependencies of ventilation intensity on wave period observed in transit operation and at bollard. Hydrodynamic interaction between the components of forced propulsor motion plays an important role in the resulting changes in propulsor forces and their oscillations. The combined motion (heave+sway+roll) reveals generally larger force oscillations compared to individual motion components.

References

Berchiche, N., Krasilnikov, V.I., and Koushan, K. (2018), "Numerical Analysis of Azimuth Propulsor Performance in Seaways: Influence of Oblique Inflow and Free Surface." Journal of Marine Science and Engineering, 2018, 6, 37; doi:10.3390/jmse6020037.

Dang, J., Koning, J., Brouwer, J. and de Jong, J. (2013), "Dynamic Loads on Mechanical Azimuth Thrusters." Proceedings of the PROADS2013, CECO, Changwon City, Korea, October 20-25.

Koushan, K. (2006b), “Dynamics of Propeller Blade and Duct Loadings on Ventilated Ducted Thrusters Operating at Zero Speed.” Proceedings of T-POD06 - 2nd International Conference on Technological Advances in Podded Propulsion, Brest, France.

Krasilnikov, V.I., Berchiche, N., and Koushan, K. (2019), "Thrust Losses and Dynamic Loads on a Ducted Pushing Thruster in Regular Waves.", Proceedings of the 6th International Symposium on Marine Propulsors SMP'19, Rome, Italy, May.